Thermomagnetic Convection-Surface Radiation Interactions in Microgravity Environment

Saber Hamimid[1] and Messaoud Guellal[2]

Abstract   The numerical study of combined thermo-magnetic convection and surface radiation is presented in this paper and computations are performed for a paramagnetic fluid filled square cavity whose four walls have the same emissivity, placed in a microgravity environment (g ≈0), and subjected to various strong non-uniform magnetic field gradients. The vertical walls were isothermal, and the horizontal walls were adiabatic. Finite volume method based on the concepts of staggered grid and SIMPLER algorithm has been applied, and the view factors were determined by analytical formula. Representative results, illustrating the effect of magnetic field strength on streamlines, temperature contours and Nusselt numbers, show that temperature differences occur within the cavity giving rise to convectif motion of the paramagnetic fluid which takes place even in a zero-gravity environment.

Keywords: thermomagnetic convection, surface radiation, Numerical simulation, microgravity, Paramagnetism, Magnetizing force.

Nomenclature

A_i	=	radiative surface number i
A_{ij}	=	Elements of matrix A
Cp	=	specific heat at constant pressure, $J.kg^{-1}.k^{-1}$
F_{ij}	=	geometry view factor
F_{Kelvin}	=	Magnetizing force, N
g	=	gravitational acceleration, $m.s^{-2}$
H	=	size of the enclosure, m
J_i	=	dimensionless radiosity of surface A_i
k	=	thermal conductivity, $W.m^{-1}.K^{-1}$
N	=	total number of radiative surfaces
Nr	=	Radiation-conduction number, $\sigma T_0^4 (k\,\Delta T\,/\,H)$
Nu_c	=	Convective Nusselt number

[1] Dr. Saber Hamimid, Faculty of Sciences and Applied Sciences, sa_hamimid@yahoo.fr.
[2] Pr. Messaoud Guellal, Laboratory for Chemical Engineering, messaoud.guellal@gmail.com.

Nu_r	=	Radiative Nusselt number
Nu_t	=	total Nusselt number
p	=	fluid pressure , Pa
p'	=	perturbation pressure , Pa
p_0	=	static pressure , Pa
P	=	dimensionless pressure,
Pr	=	Prandtl number, ν / α .
q_r	=	net radiative flux ($W.m^{-2}$)
Q_r	=	dimensionless net radiative-flux, $q_r / \sigma T_0^4$
Ra_m	=	Magnetic Rayleigh number, $\chi_0 B_0^2 \beta \Delta T H^2 / \mu_m \nu \alpha$
t	=	Time, s
T	=	dimensional temperature, K
$T_H(T_C)$	=	temperature on left (right) vertical wall of cavity, K
T_0	=	Reference temperature, $(T_C - T_H)/2$, K
u	=	Velocity in x-direction ,$m.s^{-1}$
v	=	Velocity in y-direction, $m.s^{-1}$
U, V	=	dimensionless velocity-components, $m.s^{-1}$
x, y	=	cartesian coordinates, m
X, Y	=	dimensionless coordinates

Greek symbols

α	=	thermal diffusivity, $m^2.s^{-1}$
β	=	thermal expansion coefficient: $k^{-1}, -1/\rho_0(\partial\rho/\partial T)$
χ	=	specific magnetic susceptibility,
χ_m	=	volumetric magnetic susceptibility, m^3/kg
ΔT	=	temperature difference, $\Delta T = T_C - T_F$, K
ε	=	emissivity of surface
μ	=	dynamic viscosity of the fluid, $Kg.m^{-1}s^{-1}$
μ_m	=	free space magnetic permeability, $H.m^{-1}$
ν	=	kinematic viscosity, $m^2.s^{-1}$
ψ	=	dimensionless stream function
ρ	=	fluid density, $Kg.m^{-3}$
σ	=	Stefan–Boltzmann constant, $W.m^{-1}.K^{-4}$
Θ	=	dimensionless temperature, T/T_0
δ_{ij}	=	Kronecker symbol

θ =   dimensionless temperature, $(T - T_0)/\Delta T$.

τ =   dimensionless time

<u>Subscripts</u>

avg	=	average value
max	=	maximum value
b	=	bottom
mid	=	midplan
min	=	minimum value
0	=	reference state
C	=	cold
c	=	convective
H	=	hot
r	=	radiative
t	=	top

1   Introduction

The effects of surface radiation on free convection in enclosures exposed to terrestrial gravitational field, where differences in fluid density between hot and cold regions are due to buoyancy force, have been studied by many investigators and it has been a very widespread research topic for many years. In a zero-gravity environment, there can be no buoyancy forces and thus no natural (free) convection possible, so flames in many circumstances without gravity smother in their own waste gases.

Researches and applications in magnetic fields have significantly increased in recent years. The development of superconducting magnets has allowed the generation of magnetic fields up to 20 T (or higher with hybrid magnets). The magnetic field affects the convection of both electroconducting fluids (liquid metals) and non-electro-conducting fluids (the diamagnetic and paramagnetic fluids).

A pioneering work in this area is of Braithwaite et al. (1991), who described the suppression or enhancement of gravitational convection of paramagnetic fluid by a magnetic field. Many experimental and numerical researches works have followed, e.g. Tagawa et al. (2002), Shigemitsu et al. (2003), and Bednarz et al. (2005). A major contribution of these studies was in providing the integral heat transfer (Nusselt number) behavior under strong magnetic fields and in reporting some basic flow visualizations.

It has been demonstrated that strong magnetic fields modify the shape of candle flames and smokes in the air [Wakayama (1991), Wakayama (1993), Ueno (1989),] and can levitate water at 20T or over by diamagnetic levitation Beaugnon and Tournier (1991). Water can splits into two parts by the application of magnetic field, Ueno and Iwasaka (1994).

Flow modes as well as heat transfer characteristics of natural convection of magnetic fluids have always attracted researchers' attention in many fields of science and engineering. Particulary, magnetic fluids are promising in the space engineering where the gravity acceleration can be replaced by the magnetic body force. [Rosensweig (1954),

Berkovsky (1993)]. Maki et al. (2002) evidenced the similarity between gravity convection and magneto-gravity convection induced within air by a vertical magnetic field gradient.

Yang et al. (2003) numerically studied the air free convection induced by a magnetic quadrupole field under microgravity, and indicated that free convection induced by the centrifugal- form magnetic force presents different flow and heat transfer behavior from the gravitational natural convection. In this work, the magnetic quadrupole field is used to enhance the forced convection of air. The flow and heat transfer behaviors in the presence of the magnetic quadrupole field are presented and discussed.

Few studies have examined the interaction between natural convection and surface radiation in the case of a differentially heated cavity, particularly in terrestrial state either for a Boussinesq conditions, Hamimid and M.Guellal (2014) or under non-Boussinesq conditions, Hamimid et *al.* (2015).

However, the interaction between thermomagnetic convection and surface radiation is rarely studied although surface radiation is inherent in natural convection; it appears that no work was reported on coupled thermomagnetic convection and radiation in the case of micro-gravity in a differentially-heated square cavity. Thereafter, due to its practical interest, the subject needs further effort to improve the knowledge in this field.

In this study, we propose to extend the analysis of this interaction between a paramagnetic fluid convection and surface radiation in a square cavity with differentially heated vertical walls in case of micro-gravity conditions where the driving force is the Magnetizing force produced by the gradient magnetic field. The main objective of the present study consists of examining the effect of the emissivity of walls on fluid flow and heat transfer.

2   Mathematical formulation

2.1   Governing equations

Details of the considered geometry are shows in fig.1. The flow is assumed to be incompressible, laminar and two dimensional in a square cavity; the two horizontal walls are perfectly insulated, while the two vertical walls are maintained at different temperatures T_H and T_C , respectively. It will be further assumed that the cavity is placed inside a vertical superconducting magnet (Fig. 1). The temperature differences in the domain under consideration are small enough to justify the employment of the Boussinesq approximation. Moreover, the spatial variations of the magnetic fields are modeled using Gaussian profiles in the following forms in case of a vertical gradient of the magnetic field, Tonino et *al.* (2005):

$$b(y) = b_0 e^{-\lambda(y-y_m)^2} \tag{1}$$

where:

$$\lambda = -4Ln(10^{-2}) \tag{2}$$

y_m represents the ordinate of the point where the magnetic field is maximum.
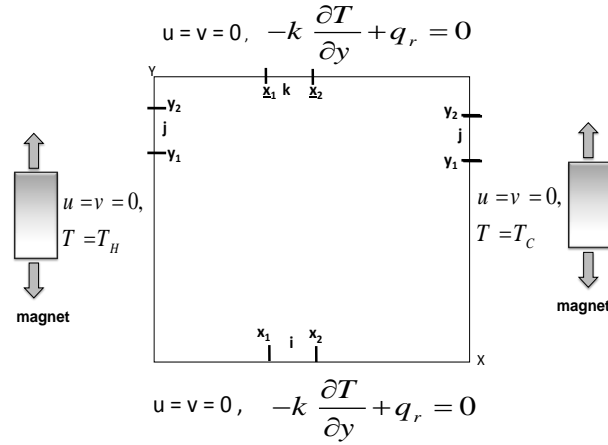
Figure 1: Flow configuration and coordinate system.

The fluid is air and its properties are assumed to be constant at the average temperature. The inner surfaces, in contact with the fluid, are assumed to be gray, diffuse emitters and reflectors of radiation with identical emissivities.

The application of a magnetic field gradient produces a force (Kelvin force) given as follows, McGraw-Hill (1992):

$$\overrightarrow{F}_{kelvin} = \frac{\chi_m(T)}{2\mu_m}\nabla b^2 = \frac{\rho\chi(T)}{2\mu_m}\nabla b^2 \tag{3}$$

The magnetizing force is in the direction of gradient of b and does not coincide with the direction of b.

This can be included as a body force in the Navier-Stokes equation for a vertical magnetic gradient as follows:

$$\rho(\frac{\partial v}{\partial t} + u\frac{\partial v}{\partial x} + v\frac{\partial v}{\partial y}) = \frac{\rho\chi}{2\mu_m}\frac{\partial b^2}{\partial y} - \frac{\partial p}{\partial y} + \mu(\frac{\partial^2 v}{\partial x^2} + \frac{\partial^2 v}{\partial y^2}) \tag{4}$$

(here $g = 0$, zero gravity situation)

where μ_m is the free space magnetic permeability ($4\pi \times 10^{-7}$ H/m in SI units), b is the magnetic field intensity, χ_m is the volumetric magnetic susceptibility and satisfies $\chi_m = \rho\chi$

ρ is the density and χ is the specific magnetic susceptibility. According to Curie's law, the magnetic susceptibility (χ) of a paramagnetic material is inversely proportional to its absolute temperature, W. E (1835).

$$\chi = \frac{C}{T} \tag{5}$$

where C is the Curie's constant.

If the Taylor expansion for the Curie's law is introduced, Yang et *al.* (2003), we can derive a Boussinesq approximation for this force term, [Tagawa et *al.* (2003), Tagawa et al. (2002].

$$\vec{F}_{kelvin} = \frac{-\beta\rho_0\chi_0(T - T_0)}{\mu_m}\nabla b^2 \tag{6}$$

Taking into account the assumptions mentioned above, the governing equations for this problem are the Navier-Stokes equations for fluid flow, including the magnetic force f_{Kelvin} given by equation 6; the complete set of equation is:

$$\nabla.V = 0 \tag{7}$$

$$\rho\left(\frac{\partial u}{\partial t} + u\frac{\partial u}{\partial x} + v\frac{\partial u}{\partial y}\right) = -\frac{\partial p'}{\partial x} + \mu\left\{\frac{\partial^2 u}{\partial x^2} + \frac{\partial^2 u}{\partial y^2}\right\} \tag{8}$$

$$\rho\left(\frac{\partial v}{\partial t} + u\frac{\partial v}{\partial x} + v\frac{\partial v}{\partial y}\right) = -\frac{\partial p'}{\partial y} + \mu\left(\frac{\partial^2 v}{\partial x^2} + \frac{\partial^2 v}{\partial y^2}\right) - \frac{\beta\rho_0\chi_0(T - T_0)}{\mu_m}\nabla b^2 \tag{9}$$

$$\frac{\partial T}{\partial t} + u\frac{\partial T}{\partial x} + v\frac{\partial T}{\partial y} = a\left(\frac{\partial^2 T}{\partial x^2} + \frac{\partial^2 T}{\partial y^2}\right) \tag{10}$$

Where $p' = p - p_0$ is the perturbation pressure.

We used H , H^2/α, $\frac{\alpha}{H}$, $\frac{\rho\alpha^2}{H^2}$ and b_0 as characteristic scales for length, time, velocity, pressure and magnetic field, respectively. The non-dimensional temperature is defined as $\theta = \frac{T - T_0}{\Delta T}$. Accordingly, the dimensionless governing equations are:

$$\frac{\partial U}{\partial X} + \frac{\partial V}{\partial Y} = 0 \tag{11}$$

$$\frac{\partial U}{\partial \tau} + U\frac{\partial U}{\partial X} + V\frac{\partial U}{\partial Y} = -\frac{\partial P}{\partial X} + \Pr(\frac{\partial^2 U}{\partial X^2} + \frac{\partial^2 U}{\partial Y^2}) \tag{12}$$

$$\frac{\partial V}{\partial \tau} + U\frac{\partial V}{\partial X} + V\frac{\partial V}{\partial Y} = -\frac{\partial P}{\partial Y} + \Pr\left\{\frac{\partial^2 V}{\partial X^2} + \frac{\partial^2 V}{\partial Y^2}\right\} - Ra_m.\Pr\theta\frac{\partial B^2}{\partial Y} \tag{13}$$

$$\frac{\partial \theta}{\partial \tau} + U\frac{\partial \theta}{\partial X} + V\frac{\partial \theta}{\partial Y} = (\frac{\partial^2 \theta}{\partial X^2} + \frac{\partial^2 \theta}{\partial Y^2}) \tag{14}$$

Where $Ra_m = \frac{\chi_0 B_0^2\beta\Delta T H^2}{\mu_m\nu\alpha}$ is magnetic Rayleigh number.

2.2 *Radiative analysis*

The radiative surfaces of the enclosure are divided into N elementary zones A_i, i = 1,. ..N. N is equal to the total control volume solid–air interfaces. In fact, the control volume faces were arranged so that a control volume face coincided with an interface solid–fluid. Surfaces A_i are assumed to be diffuse-gray and opaque.

The number of zones retained was determined by the mesh used to solve the differential equations. Indeed, the grid was constructed such that the boundaries of physical domain coincided with the velocity grid lines.

Determination of the net radiative flux density requires the knowledge of the surface temperature of each node. The equation of the thermal balance of each surface provides us with these temperatures. Thus, one assumes that the solid surfaces are in thermal equilibrium under the combined action of the convective and radiative contributions, which give:

$$-k\frac{\partial T}{\partial n} + q_r = 0 \tag{15}$$

Where n denotes the normal direction to the interface under consideration. and q_r the net radiative flux density along this interface.

The corresponding initial and boundary conditions are:

$$U = V = 0 \, , \quad \theta = \theta_i \qquad \text{for} \quad \tau = 0$$

$$U = V = 0 \, , \quad \theta = \theta_C = -0.5 \quad \text{for} \quad 0 \leq Y \leq 1 \text{ at } X = 0$$

$$U = V = 0 \, , \quad \theta = \theta_H = 0.5 \quad \text{for} \quad 0 \leq Y \leq 1 \text{ at } X = 1$$

$$U = V = 0 \, , \quad \frac{\partial \theta}{\partial Y} - NrQ_r = 0 \quad \text{for} \quad 0 \leq X \leq 1 \text{ at } Y = 0$$

$$U = V = 0 \, , \quad \frac{\partial \theta}{\partial Y} - NrQ_r = 0 \quad \text{for} \quad 0 \leq X \leq 1 \text{ at } Y = 1$$

For the insulated walls:

$$\left.\frac{\partial \theta}{\partial Y}\right|_{Y=0,1} - N_r Q_r\Big|_{Y=0,1} = 0 \tag{16}$$

Where $Nr = \sigma T_0^4 H / k\,\Delta T$, is the dimensionless parameter of conduction-radiation and $Q_r = q_r / \sigma T_0^4$, is the dimensionless net radiative heat flux on the corresponding insulated wall defined as follows:

$$Q_{r,i} = J_i - \sum_{j=1}^{N} J_j F_{i-j} \tag{17}$$

J_i is the dimensionless radiosity of surface A_i , obtained by resolving the following system:

$$\sum_{j=1}^{N} (\delta_{ij} - (1-\varepsilon_i)F_{i-j})J_j = \varepsilon_i \Theta_i^4 \tag{18}$$

Where the dimensionless radiative-temperature Θ_i is given by:

$$\Theta_i = \frac{T_i}{T_0} = \frac{\theta_i}{\theta_0} + 1 \tag{19}$$

2.3 Heat transfer

The local non-dimensional heat transfer rate in terms of convective and radiative Nusselt numbers, Nu_c and Nu_r, are given by:

$$Nu_c = \frac{\partial \theta}{\partial Y} \tag{20}$$

$$Nu_r = N_r Q_r \tag{21}$$

The average convective Nusselt number was calculated integrating the temperature gradient over surface A as

$$Nu_{c_{avg}} = \frac{1}{A} \int_0^A -\frac{\partial \theta}{\partial Y} dY \tag{22}$$

The average radiative Nusselt number was obtained integrating the dimensionless net radiative fluxes over surface A, by the following mathematical relationship

$$Nu_{r_{avg}} = N_r \frac{1}{A} \int_0^A Q_r dY \tag{23}$$

The total average Nusselt number was calculated by summing the average convective Nusselt number and the average radiative Nusselt number

$$Nu_{avg} = \frac{1}{A} \int_0^A \left(-\frac{\partial \theta}{\partial Y} + N_r Q_r \right) dY \tag{24}$$

2.4 Numerical procedure

The numerical solution of the governing differential equations for the velocity, pressure and temperature fields is obtained by using a finite volume technique. A power scheme interpolates the face value of a variable,Φ, using the exact solution to a one-dimensional convection-diffusion equation was also used in approximating advection–diffusion terms.This scheme is based on the analytical solution of the convection diffusion equation. This scheme is also very effective in removing false diffusion error [Patankar (1980)]. The SIMPLER algorithm (Semi-Implicit Method for Pressure Linked Equations Revised) whose details can be found in Patankar (1980), with a staggered grid is employed to solve the coupling between pressure and velocity. The governing equations were cast in transient form and a fully implicit transient differencing scheme was employed as an iterative procedure to reach steady state. The discretised equations are solved using the line by line Thomas algorithm with two directional sweeps. The radiosities of the elemental wall surfaces are expressed as a function of elemental wall surface temperature, emissivity and the view factors. The radiosity (J_j) and temperature

(Θ_i) are connected by a matrix of the type

$$\left[A_{i,j} \right]\left\{ J_j \right\} = \left\{ \varepsilon_i \Theta_i^4 \right\}$$
(25)

The inverse of the matrix $[A_{i,j}]$ is determined (only once) by the Gauss elimination method. The coefficients of $[A]$ are constants and depend only on the emissivity and the view factors. They have no dependence on the temperatures. In 2D, the view factors are analytic, (see details in fig.1) :

$$F_{i-j} = \frac{-1}{2(x_2 - x_1)} \left[\left. \sqrt{x_2^2 + y^2} \right|_{y_1}^{y_2} - \left. \sqrt{x_2^2 + y^2} \right|_{y_1}^{y_2} \right]$$
(26)

$$F_{i-k} = -\frac{1}{2(x_2 - x_1)} \left[\left. \sqrt{(\underline{x}_2 - x)^2 + H^2} \right|_{x=x_1}^{x=x_2} - \left. \sqrt{(\underline{x}_1 - x)^2 + H^2} \right|_{x=x_1}^{x=x_2} \right]$$
(27)

3   Validation

The lack of the experimental and numerical data for thermomagnetic convection surface radiation coupling especially for micro gravity environment has motivated this study. There is little data in the literature dealing with zero-gravity thermomagnetic convection-surface radiation interactions. We therefore considered two cases for validation; for the first validation test a case of natural convection coupled with surface radiation in differentially heated square cavity studied by Hong (2006) was used for this test case.

For the second validation test, we have made calculation for the flow in the case of thermomagnetic convection in a differentially heated square cavity under conditions which resemble those used by Tonino et al (2005).

Table 1: average values of *convective*, *radiative and total Nusselt numbers on the hot wall for* $T_0 = 293,5$ K *and* $\Delta T = 10K$, *Nut = Nuc + Nur.* Comparison with the values published by Hong (2006).

Ra	H	ε	Hong et *al.* (2005)			Present study		
			Nu_c	Nu_r	Nu_t	Nu_c	Nu_r	Nu_t
10^4	0.021	0	2.246	0	2.246	2.246	0	2.246
10^4	0.021	0.2	2.260	0.507	2.767	2.262	0.507	2.769
10^4	0.021	0.8	2.249	2.401	4.650	2.255	2.401	4.656
10^5	0.045	0	4.540	0	4.540	4.532	0	4.532
10^5	0.045	0.2	4.394	1.090	5.484	4.398	1.090	5.489
10^5	0.045	0.8	4.189	5.196	9.385	4.200	5.196	9.397
10^6	0.097	0	8.852	0	8.852	8.863	0	8.863
10^6	0.097	0.2	8.381	2.355	10.736	8.379	2.355	10.734
10^6	0.097	0.8	7.815	11.265	19.080	7.861	11.265	19.126

Table 2: average nusselt number for $Ra = 10^5$ and different values of Gm. Comparison with the values published by Tonino (2006).

Gm	0	2.5×10^5	10^6	4×10^6	9×10^6	1.6×10^7	2.5×10^7
Nu_C :Tonino (2006)	4.525	4.522	4.480	3.8	5.305	6.649	7.635
$\boldsymbol{Nu_C}$: present study	4.522	4.520	4.485	3.82	5,57	6.686	7.616

Tonino (2006)

Present study

| Gm | 0 | 10^6 | 4×10^6 | 2.5×10^7 |
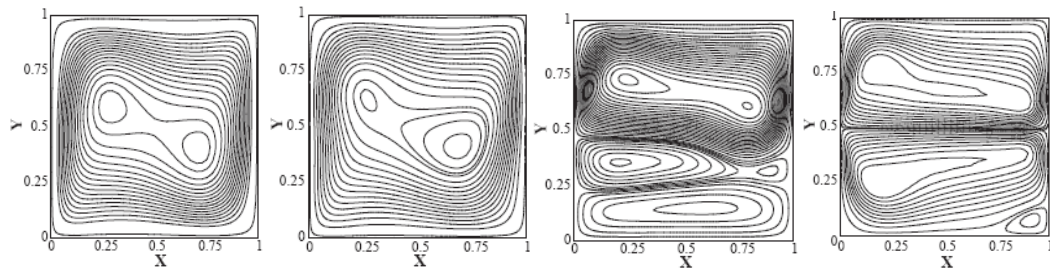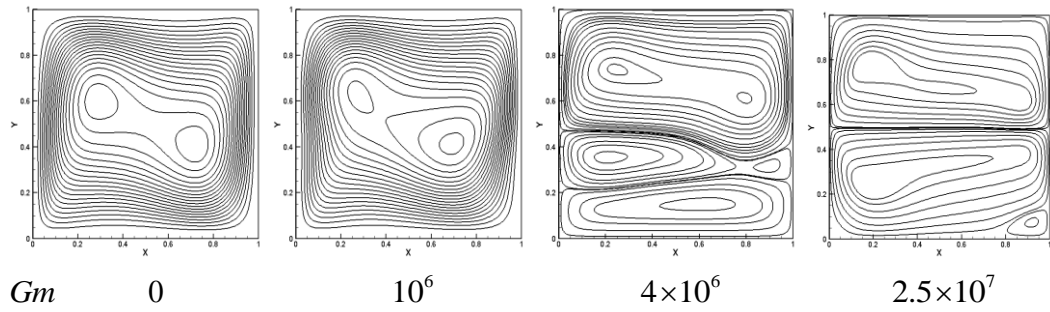
Figure 2: streamlines for $Ra = 10^5$ and different values of Gm.

Tonino (2006)

Present study

| *Gm* | 0 | 10^6 | 4×10^6 | 2.5×10^7 |
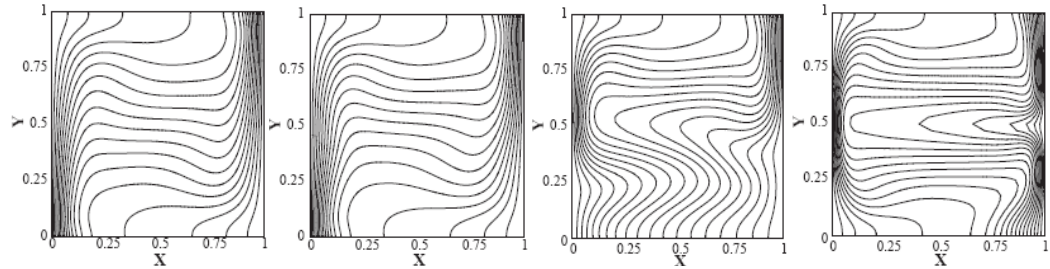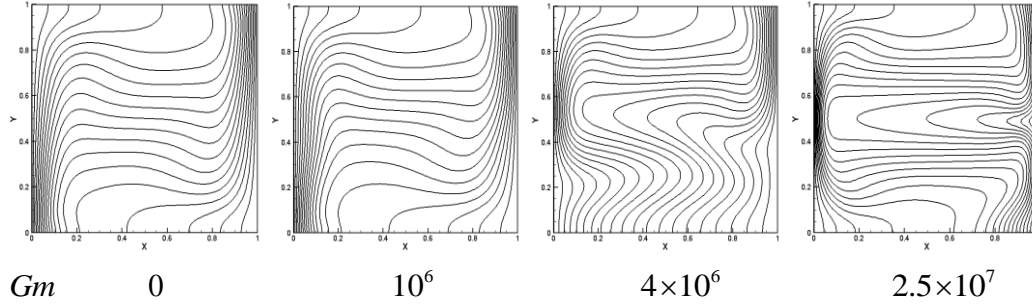
Figure 3: isotherms for $Ra = 10^5$ and different values of *Gm* .

A comparison of our numerical data with results from the literature and for these test cases is shown in figures (2,3) shows the thermal and flow structure as obtained for the particular Rayleigh number, $Ra = 10^5$ and for different *Gm* where $Gm = \dfrac{\chi_0 H^2 b^2}{\mu_m \nu^2}$ and

Tables 1 and 2, showing the mean values of Nusselt numbers. The agreement between our results and others can be qualified as quite satisfactory since the relative maximum deviation was found to be less than 2%.

We do firmly believe that the above agreement may give a confident assessment regarding our mathematical modelling as well as the numerical method adopted.

To ensure that the results are mesh-size independent, different non-uniform $n_x \times n_y$ fine near wall grid, namely 120×60 and 120×100, were thoroughly tested. The difference between results given by those grids was less than 1% for the average value of Nusselt numbers. Hence, most of the calculations presented in this article were performed using an 120×80 grid. Such a grid system possesses very fine meshes near all boundaries.

4   Results and discussion

In this investigation, thermo-magnetic convection coupled with surface radiation is studied in the case of zero gravity situations. This required the specification of five dimensionless parameters (ε , Ra_m , Nr , H and Y_m) corresponding to the emissivity of walls, magnetic Rayleigh number, the radiation number, the high of cavity and the magnet position; the others parameters such as Prandtl number, average temperature and temperature differences are respectively fixed to $Pr = 0.71$, $T_0 = 300$ K and $\Delta T = 10$ K.

The simulation parameters are: $\varepsilon = 0 \to 1$, $Ra_m = 10^6$ (corresponding to $Nr = 162.88$ and $H = 9.68 \times 10^{-2} m$) and $Y_m = (0.5,1)$.

The Kelvin force, which arises from the interaction between the local magnetic field within the fluid and the molecular magnetic moments, tends to move paramagnetic fluids toward regions of higher magnetic field.

When the cavity of a paramagnetic fluid heated from the side is placed in the non uniform magnetic field, the imposed horizontal thermal gradient induces a horizontal gradient of

the magnetic susceptibility (satisfying Curie's law), yielding a spatially non uniform Kelvin body force. This thermal gradient induced by magnetic body force tends to destabilize the fluid in the cavity and convection of the paramagnetic fluid might take place even in a zero-gravity environment, (Fig.4, 5), as a direct consequence of temperature differences occurring within the fluid. The resulting flow is therefore, illustrated by natural convection cells and isotherms contours which show the existence of strong temperature gradients near the active walls to which the magnetic field is maximum(Fig.5).

| $\varepsilon = 0$ | $\varepsilon = 0.2$ | $\varepsilon = 0.6$ | $\varepsilon = 1$ |
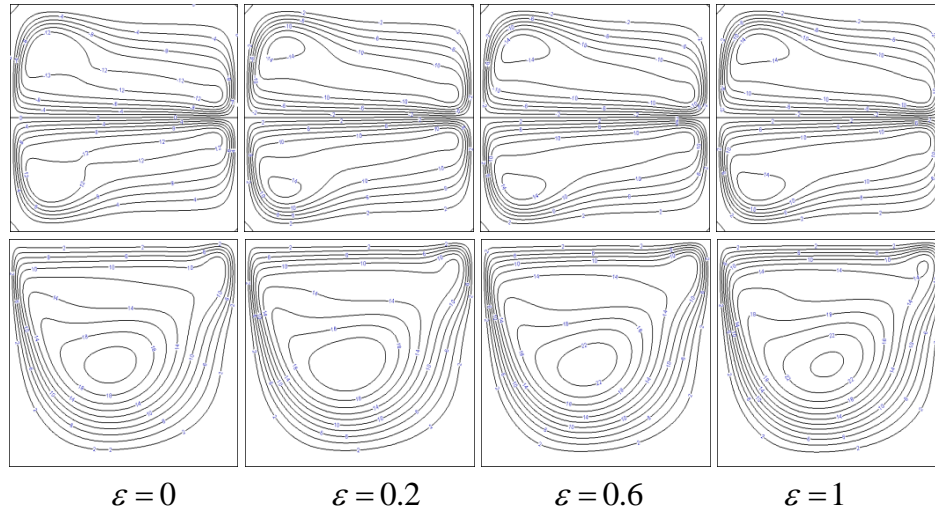
Figure 4: Streamlines for $Y_m = 0.5$ (top) and $Y_m = 1$ (bottom) at $Ra_m = 10^6$

| $\varepsilon = 0$ | $\varepsilon = 0.2$ | $\varepsilon = 0.6$ | $\varepsilon = 1$ |
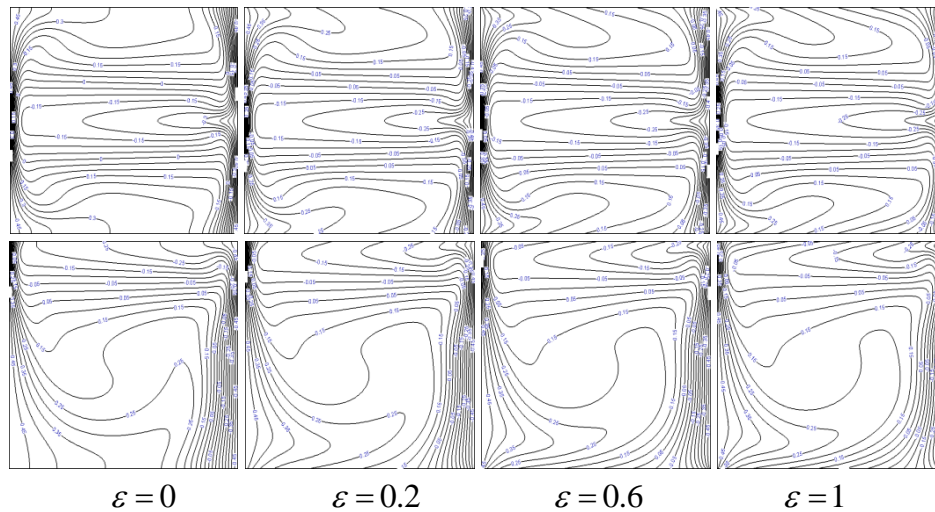
Figure 5: Isotherms for $Y_m = 0.5$ (top) and $Y_m = 1$ (bottom) at $Ra_m = 10^6$

In the presence of surface radiation, as soon as the walls emit, the radiation changes the

temperature distribution along the adiabatic walls: For a position $Y_m = 1$ of the magnet, the fluid is heated along the lower wall and cools along the upper wall, (Fig. 6b). While these two walls undergo the same change in temperature for a position $Y_m = 0.5$ of the magnet, (Fig.6a), owing to the symmetrical boundary conditions on the vertical Walls in terms of temperature and magnetic field gradient. The flow and temperature fields are symmetrical about the mid-high of the enclosure. This behavior is explained by the fact that for $Y_m = 1$ the top wall receives heat while the bottom wall loses heat, for $Y_m = 0.5$ the two walls receive the same amount of heat.

(a)   (b)
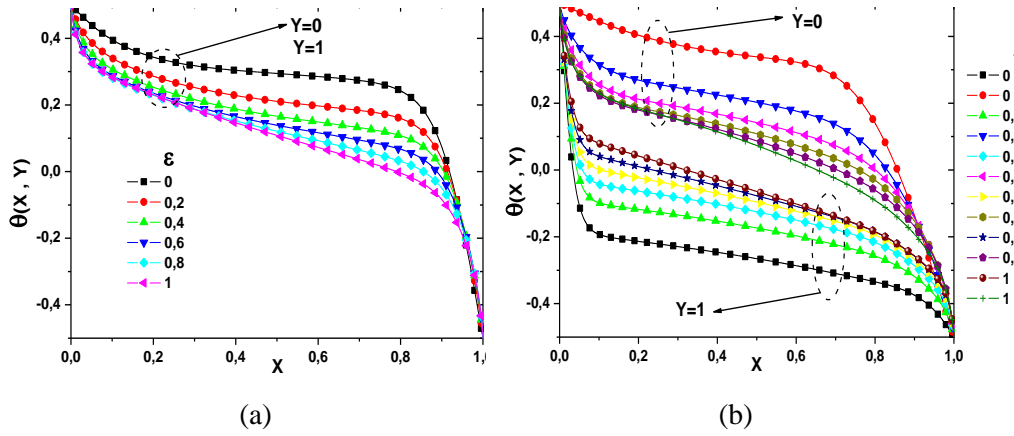
Figure 6: Distribution of upper and lower wall temperatures for $Y_m = 0.5$ (a) and

$$Y_m = 1 \text{ (b) at } Ra_m = 10^6$$

There are no significant changes in the profiles of the streamlines, (Fig.4), except a small modification in maximum values for positions $Y_m = 0.5$ and $Y_m = 1$ of the magnet, (Fig.7). Contrary to isotherms, (Fig.5), where a large change is observed especially near the adiabatic walls where the isotherms becomes more and more inclined by increasing the emissivity of the walls whereas they are perpendicular in pure thermomagnetic convection. Near the cold wall, the isotherms are not too much affected by the radiation of the walls, especially for the case $Y_m = 0.5$.
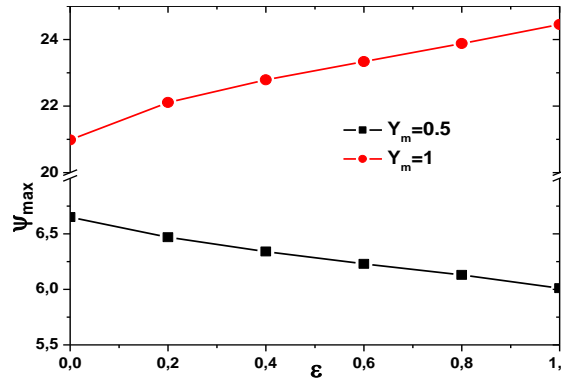
Figure 7: maximum value of the stream function for different emissivity values

Concerning the convective exchanges on the hot wall, they are greatly influenced by the radiation especially on the upper part of the wall for a position $Y_m = 1$ of the magnet, (Fig.8b). Increasing the wall emissivity ε produces a decreasing of $Nu_c(h)$ and $Nu_{cavg}(h)$ for $Y_m = 1$, (Fig.8b , Fig. 10a), whereas it is less significant for $Y_m = 0.5$ where a small increase is observed by increasing the emissivity of the walls, (Fig.8a , Fig. 10a).

For local $Nu_r(h)$ and average $Nu_{ravg}(h)$ radiative exchange, an opposite trend is observed. Increasing ε leads to an strong increase of $Nu_r(h)$ and $Nu_{ravg}(h)$ on the hot wall for the two cases: $Y_m = 1$ and $Y_m = 0.5$, (Fig.9a and Fig. 10b).

For position ($Y_m = 0.5$) of magnet, the distribution of the convective or radiative Nusselt number accepts the mid-height of the cavity as an axis of symmetry.

(a)   (b)
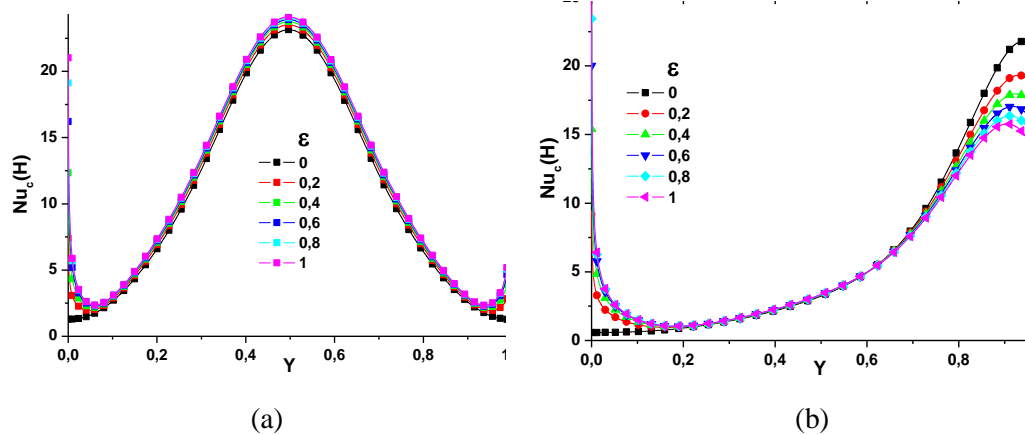
Figure 8: Distributions of local Nusselt numbers on the hot wall for $Y_m = 0.5$ (a) and $Y_m = 1$ (b) at $Ra_m = 10^6$

(a)   (b)
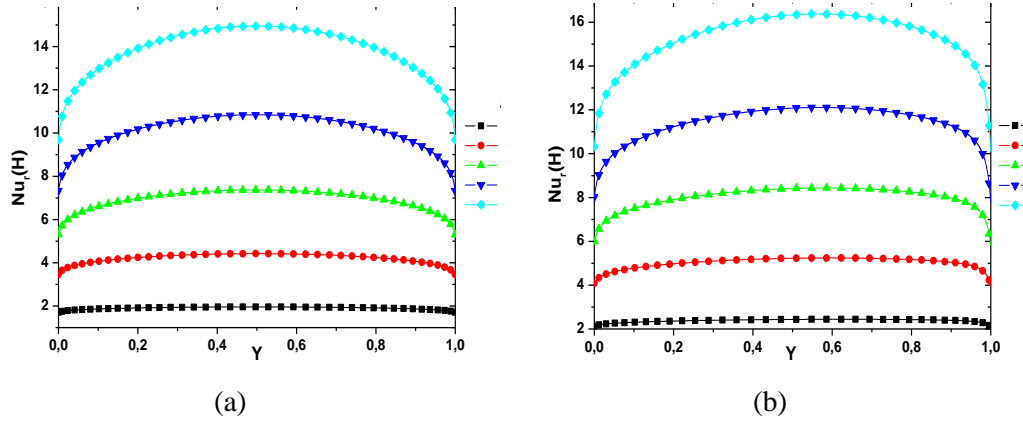
Figure 9: Variations of radiative Nusselt number at the hot and cold walls for $Y_m = 0.5$

(a) and $Y_m = 1$ (b) at $Ra_m = 10^6$

(a)   (b)
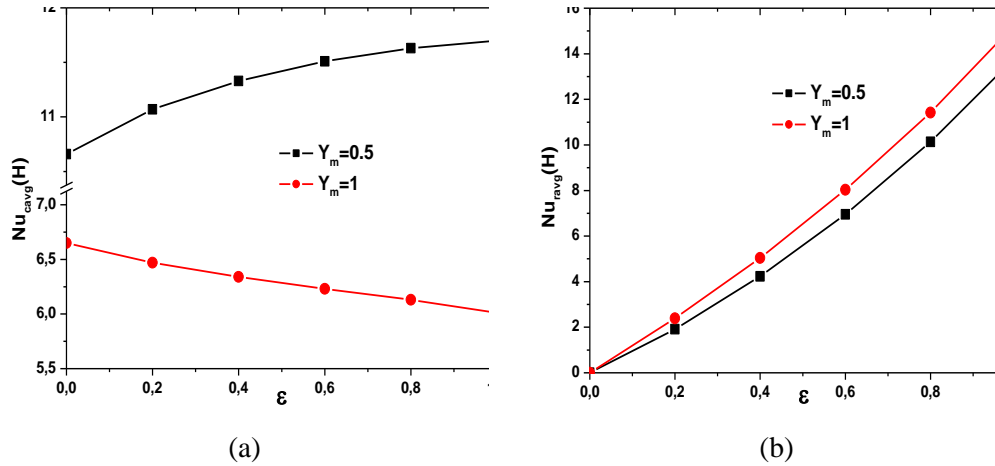
Figure 10: Variation of the average convective (a) and radiative (b) Nusselt number at
the heated surface at $Ra_m = 10^6$

Due to the symmetry of boundary conditions in terms of temperature and magnetic field, the radiative exchange to the two adiabatic walls for $Y_m = 0.5$, (Fig.11a), undergoes the same evolution and an increase in the radiative nusselt number in the greater part of walls is observed by increasing the emissivity of the walls.

For $Y_m = 1$, increasing ε leads to an increase of $Nu_r(b)$ on the bottom wall and a decrease on the top wall, (Fig.11b), and shows that the net radiative heat flux essentially positive at the bottom and negative at the top wall.
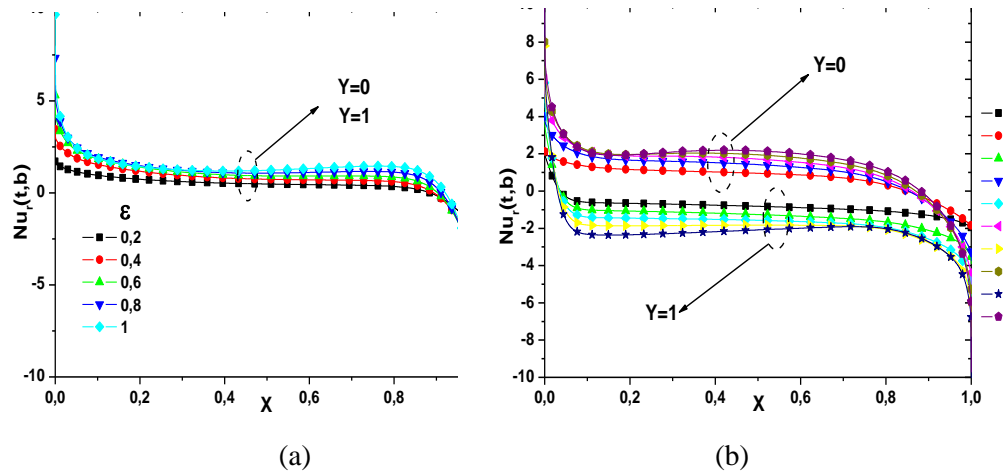
Figure 11: Distribution of radiative Nusselt number on upper and lower walls for $Y_m = 0.5$ (a) and $Y_m = 1$ (b) at $Ra_m = 10^6$

5   Conclusions

In the present paper, calculations have been made for the combined thermomagnetic convection and radiation in a differentially-heated cavity. In view of the presented results, the main points can be summarized as follows:

• In presence of the strong magnetic gradient field thermal convection of the paramagnetic fluid might take place even in a zero-gravity environment as a direct consequence of temperature differences occurring within the fluid.

• Thermal radiation affects the isotherms near solid adiabatic surfaces, since the inclination of the isotherms indicates the importance of the thermal radiation heat transfer, the modification starts at low surface emissivity and increases gradually with it.

• Varying the emissivity walls, the convective heat exchange depends on the position of the magnet, where the radiative Nusselt numbers increase with the surface emissivity.

References

Braithwaite D., Beaugnon E. and Tournier R. (1991) Magnetically Controlled Convection in a Paramagnetic Fluid. *Nature 354,* 134–136.

Bednarz T., Fornalik E., Tagawa T., Ozoe H. and Szmyd J. S. (2005) Experimental and numerical analysis of magnetic convection of paramagnetic fluid in a cube heated and cooled from opposing vertical walls. *Int. J. Thermal Sciences 44*, 933.

Beaugnon E, Tournier R (1991) Levitation of organic materials. Nature 349: 470.

Berkovsky, B. M., Magnetic Fluids Engineering Applications, 1st ed., *Oxford Univ. Press,* New York, 1993, pp. 214-228.

Hottel, H.C. (1954), Radiant heat transmission. 3 ème éd. New York, *Mc Graw-Hill Book*

Compagny.

Hamimid, S. and Guellal, M. (2014), Numerical study of combined natural convection-surface radiation in a square cavity, *FDMP*, Vol.10, no.3, PP.377-393.

Hamimid, S.; Guellal, M. and Bouafia, M. (2015), "Numerical Simulation of Combined Natural Convection Surface Radiation for Large Temperature Gradients", *Journal of Thermophysics and Heat Transfer*, Vol. 29, No. 3, pp. 636-646.

Maki, S.; Tagawa, T. and Ozoe, H. (2002), Enhanced convection or quasi-conduction states measured in a super-conducting magnet for air in a vertical cylindrical enclosure heated from below and cooled from above in a gravity field, *J. Heat Transfer* 124, 667–673.

McGraw-Hill, (1992), Encyclopedia of science and Technology, seventh ed., *McGraw-Hill,* New York.

Patankar, S.V. (1980), Numerical heat transfer and fluid flow. *Hemisphere, Washington, D.C., U.S.A*.

Rosensweig, R. E. (1954), Ferrohydrodynamics, 1st ed., Cambridge Monographs on Mecanics and Applied Mathematics, *Cambridge Univ. Press*, New York, pp. 74-98.

Shigemitsu R., Tagawa T. and Ozoe H. (2003) Numerical computation for natural convection of air in a cubic enclosure under combination of magnetizing and gravitational forces. *Numerical Heat Transfer*, Part A **43**, 449.

Tagawa T., Shigemitsu R. and Ozoe H. (2002) Magnetization force modeled and numerically solved for natural convection of air in a cubic enclosure: effect of the direction of the magnetic field. *Int. J. Heat and Mass Transfer **45***, 267.

Tagawa, T.; Shigemitsu, R. and Ozoe, H. (2003), Numerical computation for Rayleigh Benard convection of water in a magnetic field, *Int. J. Heat Mass Trans*. 46, 4097.

Tonino, S. ; Sadat, H. and Gbahoue, L. (2005), Convection thermomagnétique dans une cavité différentiellement chauffée. *Int. Commun. Heat. Mass.*, Vol. 32, pp. 923–930.

Ueno, S. (1989), Quenching of Flames by Magnetic Fields, Journal of Applied Physics, Vol. 65, No. 3, pp. 1243-1245.

Ueno, S. and Iwasaka, M. (1994), Properties of diamagnetic fluid in high gradient magnetic fields, *J. Appl. Phys.* Vol. 75, pp. 7177-7179.

Wakayama, N. I. (1991), Behavior of Gas Flow under Gradient Magnetic Fields, *Journal of Applied Physics*, Vol. 69, No. 4, pp. 2734-2736.

Wakayama, N. I. (1993), Magnetic Promotion of Combustion in Diffusion Flames, *Combustion and Flame*, Vol. 93, pp. 207-214.

W. E. (1835), Theory and applications of molecular paramagnetisme, *Eds. E.A*, 1976.

Yang, L.J.; Ren, J.X.; Song, Y.Z. and Guo, Z.Y. (2003), Free convection of a gas induced by a magnetic quadrupole field, *J. Magn. Magn. Mater*. 261, 377–384.

Yang, L.J.; Ren, J.X.; Song, Y.Z. and Guo, Z.Y. (2003), Free convection of gas induced by a magnetic quadrupole field, *J. Magn. Magn. Mater*. 261, 377-384.